Plasmonics (2012) 7:167–173
DOI 10.1007/s11468-011-9290-8

# Seed-mediated Plasmon-driven Regrowth of Silver Nanodecahedrons (NDs)

**Haifei Lu · Haixi Zhang · Xia Yu · Shuwen Zeng · Ken-Tye Yong · Ho-Pui Ho**

Received: 1 August 2011 / Accepted: 19 September 2011 / Published online: 3 November 2011


**Abstract** We report the synthesis of silver nanodecahedrons (NDs) for extending the localized surface plasmon resonance (LSPR) of silver nanostructures from blue to green-orange (~590 nm), which will enable much wider application opportunities using common laser light sources. In our photo-assisted method, we use a light-emitting-diode (LED) to control regrowth of silver ND from precursor seeds. Highly uniform silver NDs are synthesized when the LED emission peak coincides with the LSPR peak of the seeds. A two-step process involving precursor self-transformation into silver nanoprisms and nanoplates, and subsequent photo-activated regrowth of silver NDs has been proposed. Surface-enhanced Raman scattering of silver NDs in different sizes has been studied, and the average enhancement factor for each size is estimated to be in the order of ~$10^6$.

**Electronic supplementary material** The online version of this article (doi:10.1007/s11468-011-9290-8) contains supplementary material, which is available to authorized users.

H. Lu · H. Zhang · H.-P. Ho (✉)
Department of Electronic and Engineering,
The Chinese University of Hong Kong,
Shatin, Hong Kong SAR, People's Republic of China
e-mail: hpho@ee.cuhk.edu.hk

H. Lu · H. Zhang · X. Yu · S. Zeng
Singapore Institute of Manufacturing Technology,
71 Nanyang Drive,
Singapore 638075, Singapore

S. Zeng · K.-T. Yong
School of Electrical and Electronic Engineering,
Nanyang Technological University,
50 Nanyang Avenue,
Singapore 639798, Singapore

**Keywords** Localized surface plasmon resonance (LSPR) · Silver nanodecahedron (AgND) · Photochemical synthesis · Surface-enhanced Raman scattering (SERS)

## Introduction

Noble-metal nanocrystals have received considerable attention in recent years for their size- and shape-dependent plasmonic properties, and they have been used in various application areas including photonics [1], electronics [2], catalysis [3], sensing [4], and biomedicine [5]. Highly uniform silver (Ag) nanostructures of different shapes (spheres [6], rods [7], bars [8], belts [9], wires [10], prisms [11], disks [12]) have been widely reported in the literatures. It is interesting to note that plasmonic applications associated with the longer wavelength region (e.g., 500 nm and above) of the visible spectrum is largely covered by gold (Au) nanoparticles (NP)—instead of silver nanoparticles—despite that gold offers relatively lower field enhancement factors because of higher losses. Until now, reported cases of AgNPs primarily cover the UV-blue region. This impedes widespread applications of AgNPs. With the aim of extending the wavelength of localized surface plasmon resonance (LSPR) in AgNPs, Xia et al. successfully synthesized silver nanocubes that have LSPR peaks in blue-green region (420–500 nm) [13, 14]. On the other hand, silver nanodecahedrons (AgNDs) should hold some promise on expanding LSPR wavelength further in to the red region. Because of their sharp corners/edges, AgND solutions demonstrate remarkable optical properties including narrow scattering peaks and highly reproducible transmission spectra [15, 16]. Despite such special optical properties, literature reporting the growth of AgNDs is quite limited. Earlier works on the synthesis of AgNDs

using photochemical [15, 17] or *N*, *N*-dimethylformamide (DMF) reduction [18] methods have been reported by several groups. Kitaev et al. reported that growth of nanodecahedrons in a mixture of NP seeds and precursor solution can be activated by white light illumination [16]. While our experimental results indicate that a broadband light source will lead to the formation of poly-dispersive Ag nanoparticles (see Supplementary Information), it is the aim of this work to investigate the possibility of controlling the growth uniformity by using varying the wavelength of the light source. Our experiments reveal that when wavelength of the LED illumination matches with the LSPR wavelength of the AgND seeds, a seed-mediated plasmon-driven regrowth mechanism will occur, and the resultant product is highly mono-dispersive AgNDs with LSPR anywhere in the range of 489–590 nm.

## Experimental Section

### Chemicals

Silver nitrate (ACS reagent, ≥99.0%), Poly(vinyl pyrrolidone) (PVP, Mw=40,000 g/mol), L-Arginine (BioUltra, ≥99.5%), and 4-Methylbenzenethiol (98%) were purchased from Sigma-Aldrich. Sodium citrate dehydrate and sodium borohydride (99%) were purchased from Fisher Scientific. All chemicals were used with no further purification. Water used in the synthesis experiment was purified by Spectra-Teknik ultrapure water purification system. High-brightness light-emitting diodes (LEDs) with emission peaks at 465, 500, 520, and 578 nm were purchased from RS Components.

### Synthesis of Ag Nanodecahedron Seeds

Silver nanodecahedron (ND) seeds were prepared using the method reported in ref. [16]. A 0.5 mL trisodium citrate (0.05 M), 0.015 mL poly(vinyl pyrrolidone) (PVP, Mw= 40,000 g/mol, 0.05 M), 0.05 mL L-arginine (0.01 M), and 0.15 mL silver nitrate (0.005 M) were mixed with 7 mL deionized water in a clear 10 ml beaker. An 80-μL ice-cold sodium borohydride (0.1 M) was rapidly injected into the mixed solution with continuous stirring. The solution was incubated for 2 h in a dark environment at room temperature. The final bright yellow solution, which was also used for precursor in the following regrowth steps, was exposed to 465 nm radiation from a blue LED for 6 h.

### Seed-mediated Regrowth of Ag Nanodecahedrons

In a typical synthesis experiment, 2 mL AgNDs seed solution was mixed with 2–4 mL precursor solution. The final mixture was then exposed to LED illumination for 6–9 h depending on the light intensity. The spectral peak of the LED was chosen such that it was close to the LSPR peak of the ND seeds. All experiments were conducted under room temperature.

### SERS Assessment of Ag Nanodecahedrons

In a standard procedure, 100 μL AgNDs colloid after two times centrifugation wash was mixed with 900 μL 0.1 mM 4-methylbenzenethiol (4-MBT) solution in ethanol for 1 h. Then, 10 μL of the mixture was transferred to the surface of a silicon substrate and left to dry. The substrate was then rinsed by ethanol thoroughly to remove any unbounded 4-MBT. SERS measurement of single ND was conducted immediately after sample preparation. Normal Raman spectroscopy was measured with solution of 14 mM 4-MBT in NaOH (~6 M) for the calculation of average enhancement factor (EF) of the single AgND.

### Characterization

Field-emission scanning electron microscopy (FESEM) was performed using a Carl Zeiss Ultra Plus FESEM and the operating voltage was 4.96 kV. Transmission electron microscopy (TEM) images were acquired using a FEI CM120 microscope at 120 kV. The average size was determined from SEM and TEM images by averaging the edge length measurements obtained from at least 100 AgNDs. Extinction spectra were measured using a Shimadzu UV-3101 UV/Vis/NIR scanning spectrophotometer. SERS spectra were recorded using a Renishaw inVia confocal Raman spectrometer coupled to a Leica microscope. Backscattered photons were collected using a ×100 objective (NA=0.85). The 514-nm excitation source was obtained from an argon laser. The scattering spectra were recorded in the range of 550–2,000 $cm^{-1}$. Except for the normal Raman spectrum of 4-MBT, which required 20 mW and 30 s, typical accumulation time was 10 s per data point, and laser power was 1 mW.

## Results and Discussions

### Variation of LSPR Peak with Size of Silver Nanodecahedrons

Table 1 shows the extinction peak location of the final products produced from various illumination wavelengths and seed-precursor volume ratios. Extinction spectra of the products are shown in Fig. 1a, and their corresponding visual color in reflection and transmission modes are respectively shown in Fig. 1b, c. The full-width-half-maximum (FWHM) of the extinction spectra of sample 1 is about 45 nm, which indicates that the colloidal silver

**Table 1** Summary of final products obtained from exposing seed and precursor solution to LED illumination at various wavelengths

| Sample number | LED illumination peak (nm) | Seed solution volume (mL) | Precursor solution volume (mL) | Extinction peak of final silver NDs (nm) |
|---|---|---|---|---|
| 1 | 465 | N.A. | 7 | 489 |
| 2 | 500 | 2 mL sample 1 | 2 | 499 |
| 3 | 500 | 2 mL sample 1 | 3 | 516 |
| 4 | 500 | 2 mL sample 1 | 4 | 522 |
| 5 | 500 | 2 mL sample 2 | 3 | 541 |
| 6 | 500 | 2 mL sample 3 | 3 | 550 |
| 7 | 520 | 2 mL sample 4 | 4 | 562 |
| 8 | 520 | 2 mL sample 5 | 3 | 572 |
| 9 | 520 | 2 mL sample 6 | 3 | 580 |
| 10 | 520 | 2 mL sample 7 | 3 | 590 |

NDs are highly symmetric and of small size variation. Their narrow FWHM also signifies that the silver NDs may offer attractive figure-of-merit (FOM $= \frac{1}{\text{FWHM}} \bullet \frac{\Delta\omega}{\Delta n}$) [19], for sensing applications. The gradual widening of FWHM with increasing red shift is an intrinsic effect characteristic to increasing the particle size of the NDs [20]. The weak peaks nearer to the blue region can be attributed to the silver NDs' transverse resonance (see Fig. S2 in Supplementary Information) and dipole resonance of a small amount of unconsumed nanoparticles. In addition, the bi-color character (i.e., different sample colors in reflection and transmission modes) of the colloid solutions shown in Fig. 1b, c indicates that the silver NDs have low size variation and possess strong scattering coefficient in the visible region, i.e., light reflected from the colloid mainly composed of the wavelength components scattered by the silver NDs while scattered light has very limited transmission.

Figures 2a–d show the FESEM and TEM images of silver NDs with extinction peaks at 516, 522, 541, and 550 nm, respectively. Apart from a small amount of nanoprisms and nanoplates, highly uniform silver NDs make up over 90% of the products (see Fig. S3 in Supplementary Information). As shown in Fig. 3a, side view images of the silver NDs, reveal that the distance between two vertices of the two back-to-back penta-prisms is almost the same as their ridge lengths, thus indicating that the enlarged silver NDs as grown from their seeds have preserved the original shape. This is quite different from the case of silver nanodecahedrons evolving into silver pentagonal nanorods as reported in the literature [7, 21]. In such situations, strong binding of PVP to the {100} face results in preferential deposition of silver to the poorly passivated {111} face. In our regrowth experiments, with both PVP and citrate acting as surfactants, no nanorod has been found in the final solutions. It is thought that the incident optical radiation induces strong electromagnetic field at the edges, which will in turn reduce the selective binding of PVP to the {100} face, hence allowing the growth of NDs from their seeds. TEM and FESEM images of at least 100 nanoparticles have been used for estimating the average dimensions of the silver NDs, and the relationship between the major extinction peaks and the average edge lengths is shown in Fig. 3b. Quantitatively the LSPR peaks of the silver NDs, i.e., 489, 516, 522, 550,

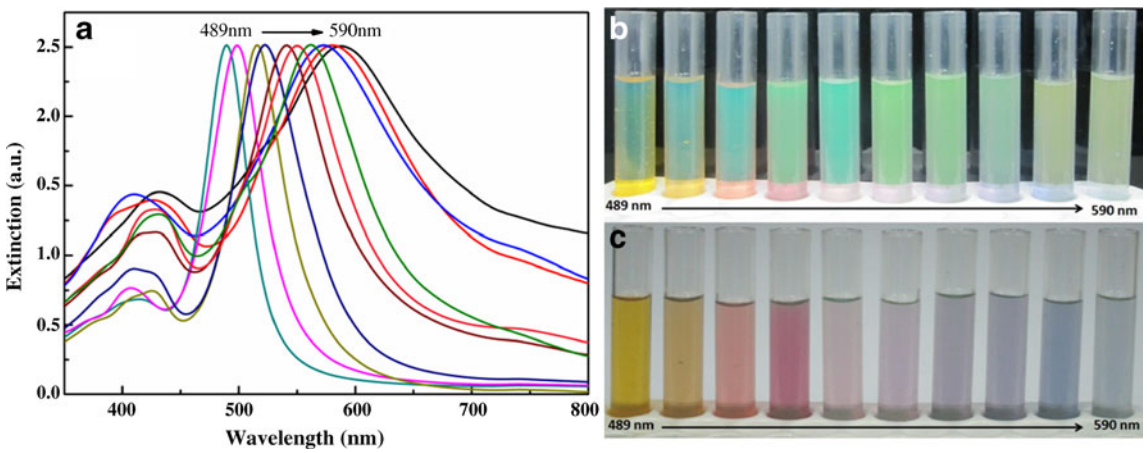


**Fig. 1** **a** UV-vis extinction spectra and photographs of final silver ND colloids taken in **b** reflected and **c** transmitted modes

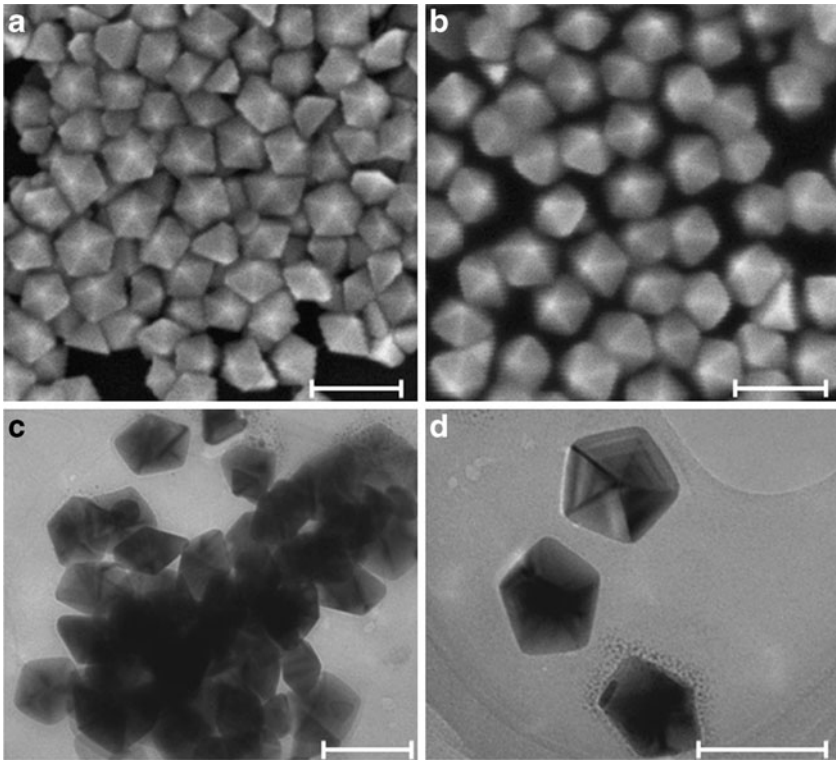


**Fig. 2** FESEM images of silver nanodecahedrons having extinction peaks at **a** 516 nm, **b** 522 nm, and TEM images of silver nanodecahedrons having extinction peaks at **c** 541 nm, **d** 550 nm. The *scale bars* in all images are 100 nm

572, and 590 nm, are related to their edge lengths (standard deviation) in the order of 28.3 (±3.6), 38.9 (±4.0), 41.7 (±4.5), 53.5 (±5.1), 61.4 (±7.6), 67.4 (±4.7) nm, respectively. (Fig. S4 in Supplementary Information shows the size distribution histograms of the silver NDs and their respective extinction peaks.) A linear relation has also been found: $l = 0.39 \times \lambda_{max} - 163.33 (R^2 = 0.998)$, where $l$ and $\lambda_{max}$ are the edge length and position of major LSPR peak, respectively.

## Regrowth Mechanism

The regrowth mechanism of our silver NDs is thought to be based on silver redox cycles, which involves reduction of $Ag^+$ on the silver ND surface under LSP excitation with the assistance of citrate and oxidative dissolution of small silver particles by $O_2$ [22]. During dipole excitation under LED illumination, a large number of hot electrons and hot holes are generated on the silver ND surface. Citrate bonding on

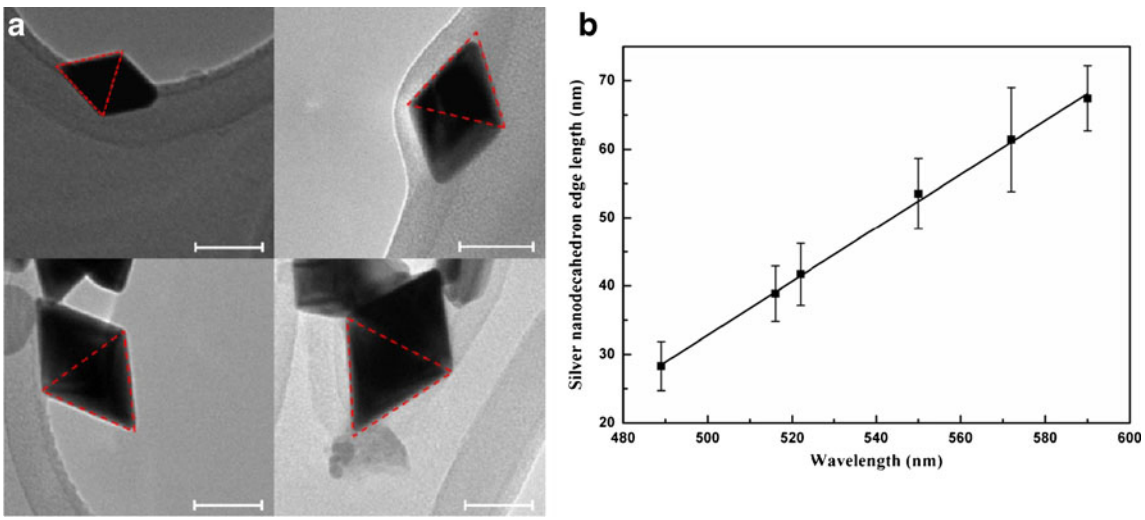


**Fig. 3** **a** TEM side view images of silver nanodecahedrons at different sizes. All *red triangles* are equilateral and the *scale bars* are 50 nm. **b** Calibration curve showing linear dependence between major localized surface plasmon resonance (LSPR) peak position and edge lengths of silver nanodecahedrons

the silver surface will be oxidized and an electron is released to neutralize the hot hole. At the same time, $Ag^+$ in the solution will receive the hot electron to become $Ag^0$, which then binds to the surface and finally results in the enlargement of silver ND. On the other hand, small silver nanoparticles introduced as precursor will be oxidized by $O_2$ to release $Ag^+$ ions, which serve as a material source for silver ND regrowth. As shown in Fig. 4, the major LSPR peak (~500 nm) of the silver NDs red shifts slowly with increasing LED illumination duration, thus suggesting the involvement of a single regrowth process during the enlargement of the silver NDs. In addition, the peak at ~400 nm decreases in intensity continuously, thus indicating that small silver nanoparticles are being consumed and gradually oxidized to form silver cations. For the small peak in the long-wavelength region (550–600 nm) during the early stage of the regrowth, we attribute this to the LSPR of small amount larger silver NDs. The seeds are quickly transformed into enlarged NDs in the presence of high concentrations of $Ag^+$ shortly after mixing with the precursor solution. As growth continues, $Ag^+$ concentration in the mixture very soon returns to a steady-state level. It should be noted that the growth of silver NDs is effectively driven by a dynamic equilibrium process, which allows the co-existence of material etching and regrowth, while the silver cation concentration in the solution is maintained. In the presence of LED irradiation, LSPR will result in the promotion of material growth. In our case, irradiation at ~500 nm will affect both small NDs with LSPR at ~516 nm as well as large NDs with LSPR in the range of 550–600 nm. Since the ~500 nm incident irradiation is close to the small NDs' LSPR peak of 516 nm, small NDs will experience much higher growth rate than that of large NDs [23]. While rapid growth of small NDs depletes silver cation concentration, the only pathway for maintaining equilibrium is to generate silver cations through oxidation of other nanoparticle species including large NDs. This phenomenon is particularly true during 5–6 h after the addition of precursor as most of the small silver nanoparticles have been consumed, and the deficiency of silver cations favors the etching of large NDs. This process will continue until the large NDs have become small enough so that their LSPR peaks are similar to that of the small NDs. This explains the observed growth in small NDs as indicated by a LSPR red shift, while large NDs undergo etching as indicated by a LSPR blue shift. In our experiment, we stop the growth process when we see that the FWHM of the extinction spectrum has reached its minimum. This typically takes 7 h.

It has been proposed in the literatures that silver precursor containing small silver nanoparticles and citrate will produce silver nanoprisms and nanoplates under the irradiation of 500 nm or longer wavelengths [15, 17, 24]. The small amount of silver nanoprisms and nanoplates found in the final product also confirms that the same reaction has taken place in our experiment. However, nanoprisms and nanoplates only amount to less than 5%. In the present case, LSP excitation has drastically increased the speed of reduction from $Ag^+$ to $Ag^0$ at the surface of the silver NDs. This leads to a much faster regrowth rate of silver NDs than the formation self-transforming seeds into nanoplates, as supported by ref. [23]. These two competitive processes, as highlighted in Scheme 1, can be controlled by the use of a light source. When LED emission peak matches with the LSPR peak of the silver ND seeds, formation of silver nanoprisms and nanoplates in the solution will be suppressed.

## LED Irradiation at Wavelength away from LSPR Peak of Silver ND Seed

Figure 5a, b are respectively the UV-vis extinction spectra of the final products obtained from exposing the reaction

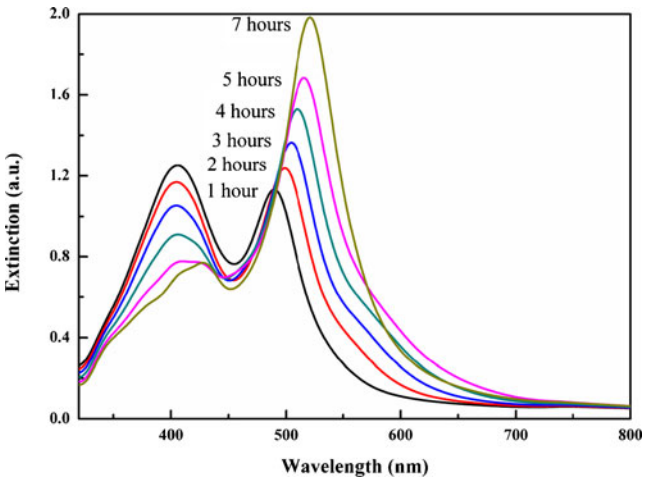


**Fig. 4** Monitoring of regrowth after exposing a reaction mixture (2 mL of silver ND seed (LSPR ~ 489 nm) solution and 4 mL of precursor solution) to 500 nm LED illumination

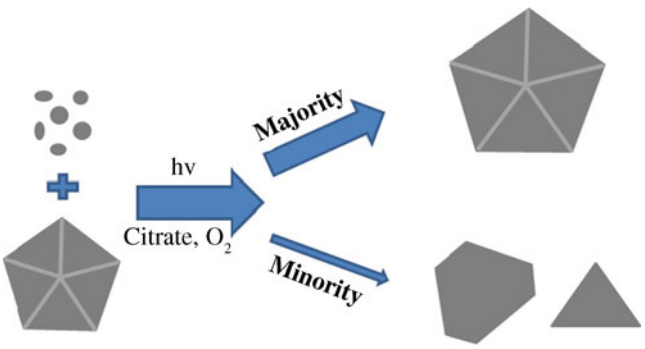


**Scheme 1** With the use of radiation close to the LSPR peak of the silver NDs seeds, regrowth of silver ND is much more favored then the formation of nanoprisms and nanoplates

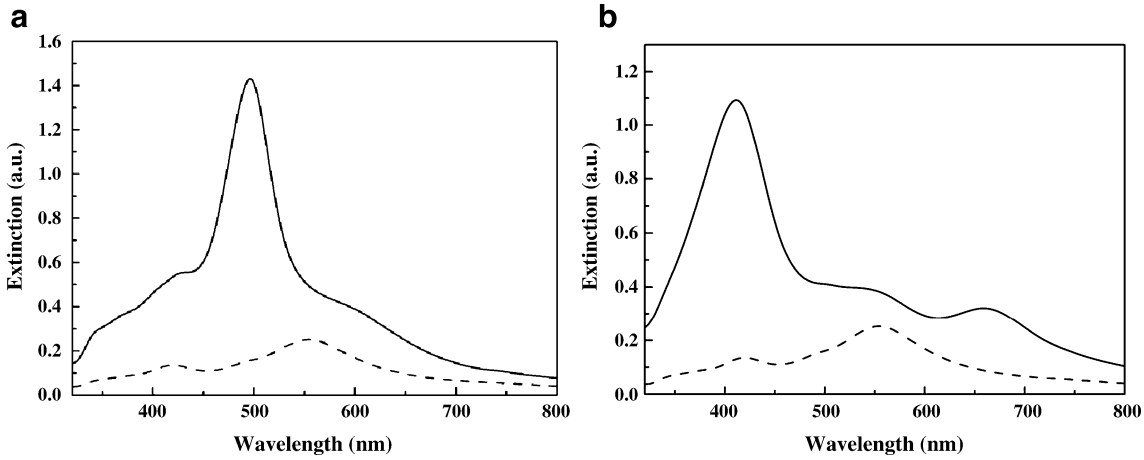


**Fig. 5** Extinction spectra of silver ND seeds (LSPR ~ 556 nm) and precursor after LED irradiation at **a** 465 nm and **b** 578 nm. *Dashed lines* are for the extinction of ND seed solutions, and *solid lines* for the final products

mixture (2 mL of silver ND seed solution (LSPR ~ 556 nm) mixed with 4 mL of precursor solution) to LED irradiation at 465 nm and 578 nm for 9 h. The 465-nm case has resulted in slight growth of the seeds and the addition of another strong peak at 496 nm. This peak belongs to newly formed silver NDs having smaller sizes, which makes the final product more poly-dispersive. For the 578-nm case as shown in Fig. 5b, the peak due to the silver ND seeds remains nearly unchanged, signifying the absence of any regrowth in the solution, while a new peak at 660 nm associated with silver nanoprisms and nanoplates has emerged. FESEM images of the product also support the presence of these nanoparticles (see Fig. S5 in Supplementary Information). The peak at around 400 nm is due to unconsumed silver nanoparticles introduced from the precursor. The reason for the observed enlargement of silver NDs seeds under 465-nm irradiation and nearly no regrowth in the 578-nm case could be attributed that photon energy of 578 nm is not sufficient to excite hot electrons and holes on the silver ND surface. Thus, little or no reduction can happen on the silver ND surface, while the only reaction to take place will be for the small silver nanoparticles to self-transform into nanoprisms and nanoplates.

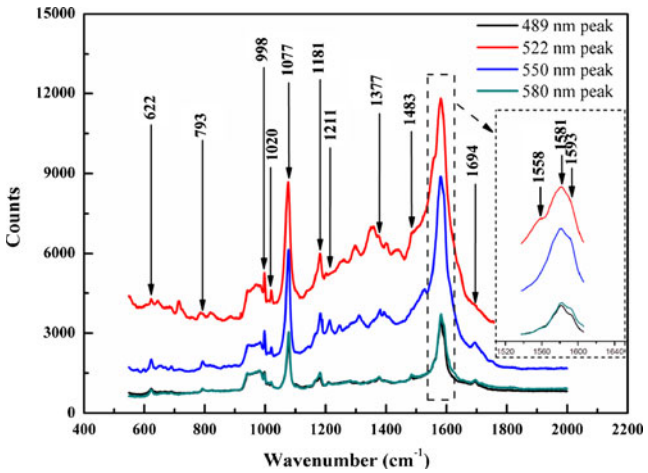


**Fig. 6** SERS spectra of individual single silver ND samples whose extinction peak are at 489, 522, 550, and 580 nm. *Dotted rectangle* region is the enlarged region of spectra within 1,537–1,606 $cm^{-1}$

## SERS Characterization of Silver Nanodecahedrons

Figure 6 shows the SERS spectra measured separately from individual samples of silver NDs whose extinction peaks are 489, 522, 550, and 590 nm. Each spectrum is obtained by averaging the spectra of 20 different sites. Majority of the Raman peaks are associated with different vibration modes of 4-MBT [25, 26]. The silicon substrate also contributes a broad peak in the 900–1,000 $cm^{-1}$ region. In order to establish the correlation between the size of the silver NDs and their SERS EF, the amplitudes of two characteristic peaks of 4-MBT at 1,077 and 1,581 $cm^{-1}$ are monitored. The method for calculating the average EF of single silver ND we adopted the equation: average $EF=(I_{sers}\times N_{bulk})/(I_{bulk}\times N_{sers})$, where $I_{sers}$ and $I_{bulk}$ are respectively the average area of the Raman peak of interest in the 20 SERS and the same Raman peak area in bulk spectra. $N_{sers}$ and $N_{bulk}$ refer to the number of molecules on a single silver ND and in the focal volume of the 14 mM 4-MBT solution, where we assume the

**Table 2** Summary of calculated average EFs of different sizes silver NDs at 1,077 $cm^{-1}$ and 1,581 $cm^{-1}$ band

| Extinction peak (nm) | Average EF (1,077 $cm^{-1}$) | Average EF (1,581 $cm^{-1}$) |
|---|---|---|
| 489 | $7.66\times10^5$ | $1.64\times10^6$ |
| 522 | $1.34\times10^6$ | $3.87\times10^6$ |
| 550 | $5.77\times10^5$ | $1.67\times10^6$ |
| 580 | $1.77\times10^5$ | $3.79\times10^5$ |

footprint of a single 4-MBT molecule on the silver surface is 0.19 $nm^2$ [27], and the focal volume of our Raman system is measured to be 10 fL according to ref. [28]. The average EFs our silver NDs possessing different extinction peaks are shown in Table 2. Silver NDs with extinction peak at 522 nm provides the largest enhancement for both Raman bands, while ND with 580 nm peak provides comparatively lower enhancement. This is due to a mismatch between the extinction peak and the Raman excitation laser wavelength (514 nm). When the irradiation wavelength from the source coincides with the resonance peak, the electric field around the silver nanoparticle under is much stronger. Since the tunability of the present approach that can provide Ag NDs with extinction peaks anywhere in the range of 489–590 nm, one can always achieve an optimal EF situation for any given Raman excitation wavelength.

## Conclusion

By controlling and tuning the mixing ratio of seed and precursor concentrations, uniform silver nanodecahedrons (NDs) with major localized surface plasmon resonance (LSPR) ranging from 489 to 590 nm have been synthesized by a seed-mediated plasmon-driven method. It is found that two processes are happening in the synthesis. The choice of LED illumination wavelength that matches with the LSP peak of the silver ND seeds can drastically suppress the formation of nanoprims and nanoplates, thus improving the uniformity of the desired nanostructures. Due to their sharp tips and edges, silver NDs provide up to $10^6$ electric field enhancement, with the possibility of further increase if one optimize the matching between the LSP peak and the irradiation laser wavelength. The reported silver NDs should find applications in biosensing and bioimaging.

**Acknowledgments** The authors thank Drs. Isakov Dmitry and Ning Ke for conducting FESEM and TEM characterizations of the samples, respectively. The project is supported by SIMTech collaborative research grant SIM/09-220001. HFL's research studentship and a Group Research Grant 3110048 from The Chinese University of Hong Kong are gratefully acknowledged.

## References

1. Maier SA (2005) Curr Nanosci 1:17
2. Li YN, Wu YL, Ong BS (2005) J Am Chem Soc 127:3266
3. Ung T, Liz-Marzan L, Mulvaney P (1999) J Phys Chem B 103:6770
4. Zeng SW, Yong KT, Roy I, Dinh XQ, Yu X, Luan F (2011) Plasmonics. doi:10.1007/s11468-011-9228-1
5. Jain PK, Huang XH, El-Sayed IH, El-Sayed MA (2007) Plasmonics 2:107
6. Evanoff DD, Chumanov G (2004) J Phys Chem B 108:13948
7. Pietrobon B, McEachran M, Kitaev V (2009) ACS Nano 3:21
8. Wiley BJ, Chen YC, McLellan JM, Xiong YJ, Li ZY, Ginger D, Xia YN (2007) Nano Lett 7:1032
9. Sun YG, Mayers B, Xia YN (2003) Nano Lett 3:675
10. Murphy CJ, Jana NR (2002) Adv Mater 14:80
11. Jin RC, Cao YC, Hao EC, Metraux GS, Schatz GC, Mirkin CA (2003) Nature 425:487
12. Chen SH, Fan ZY, Carroll DL (2002) J Phys Chem B 106:10777
13. Zhang QA, Li WY, Wen LP, Chen JY, Xia YN (2010) Chem-Eur J 16:10234
14. Zhang QA, Li WY, Moran C, Zeng J, Chen JY, Wen LP, Xia YN (2010) J Am Chem Soc 132:11372
15. Zheng XL, Zhao XJ, Guo DW, Tang B, Xu SP, Zhao B, Xu WQ, Lombardi JR (2009) Langmuir 25:3802
16. Pietrobon B, Kitaev V (2008) Chem Mater 20:5186
17. Stamplecoskie KG, Scaiano JC (2010) J Am Chem Soc 132:1825
18. Gao Y, Jiang P, Song L, Wang JX, Liu LF, Liu DF, Xiang YJ, Zhang ZX, Zhao XW, Dou XY, Luo SD, Zhou WY, Xie SS (2006) J Cryst Growth 289:376
19. Sherry LJ, Chang SH, Schatz GC, Van Duyne RP, Wiley BJ, Xia YN (2005) Nano Lett 5:2034
20. Zhou F, Li ZY, Liu Y, Xia YN (2008) J Phys Chem C 112:20233
21. Xia Y, Xiong YJ, Lim B, Skrabalak SE (2009) Angew Chem Int Edit 48:60
22. Xue C, Metraux GS, Millstone JE, Mirkin CA (2008) J Am Chem Soc 130:8337
23. Rocha TCR, Winnischofer H, Westphal E, Zanchet D (2007) J Phys Chem C 111:2885
24. Zheng XL, Xu WQ, Corredor C, Xu SP, An J, Zhao B, Lombardi JR (2007) J Phys Chem C 111:14962
25. Rycenga M, Kim MH, Camargo PHC, Cobley C, Li ZY, Xia YN (2009) J Phys Chem A 113:3932
26. Jun BH, Kim JH, Park H, Kim JS, Yu KN, Lee SM, Choi H, Kwak SY, Kim YK, Jeong DH, Cho MH, Lee YS (2007) J Comb Chem 9:237
27. Camargo PHC, Rycenga M, Au L, Xia YN (2009) Angew Chem Int Edit 48:2180
28. Le Ru EC, Blackie E, Meyer M, Etchegoin PG (2007) J Phys Chem C 111:13794